

## ORIGINAL RESEARCH

# Coronary Atherosclerosis Phenotypes in Focal and Diffuse Disease



Koshiro Sakai, MD, PhD,<sup>a,b</sup> Takuya Mizukami, MD, PhD,<sup>a,c,d</sup> Jonathon Leipsic, MD,<sup>e</sup> Marta Belmonte, MD,<sup>a,f,g</sup> Jeroen Sonck, MD, PhD,<sup>a,g</sup> Bjarne L. Nørgaard, MD, PhD,<sup>h</sup> Hiromasa Otake, MD, PhD,<sup>i</sup> Brian Ko, MD, PhD,<sup>j</sup> Bon-kwon Koo, MD, PhD,<sup>k</sup> Michael Maeng, MD, PhD,<sup>h</sup> Jesper Møller Jensen, MD, PhD,<sup>h</sup> Dimitri Buytaert, MSc,<sup>a</sup> Daniel Munhoz, MD, PhD,<sup>a,g,l</sup> Daniele Andreini, MD, PhD,<sup>m,n</sup> Hirofumi Ohashi, MD, PhD,<sup>a,o</sup> Toshiro Shinke, MD, PhD,<sup>b</sup> Charles A. Taylor, PhD,<sup>p</sup> Emanuele Barbato, MD, PhD,<sup>a,g</sup> Nils P. Johnson, MD, MS,<sup>q</sup> Bernard De Bruyne, MD, PhD,<sup>a,r</sup> Carlos Collet, MD, PhD<sup>a</sup>

## ABSTRACT

**BACKGROUND** The interplay between coronary hemodynamics and plaque characteristics remains poorly understood.

**OBJECTIVES** The aim of this study was to compare atherosclerotic plaque phenotypes between focal and diffuse coronary artery disease (CAD) defined by coronary hemodynamics.

**METHODS** This multicenter, prospective, single-arm study was conducted in 5 countries. Patients with functionally significant lesions based on an invasive fractional flow reserve  $\leq 0.80$  were included. Plaque analysis was performed by using coronary computed tomography angiography and optical coherence tomography. CAD patterns were assessed using motorized fractional flow reserve pullbacks and quantified by pullback pressure gradient (PPG). Focal and diffuse CAD was defined according to the median PPG value.

**RESULTS** A total of 117 patients (120 vessels) were included. The median PPG was 0.66 (IQR: 0.54-0.75). According to coronary computed tomography angiography analysis, plaque burden was higher in patients with focal CAD ( $87\% \pm 8\%$  focal vs  $82\% \pm 10\%$  diffuse;  $P = 0.003$ ). Calcifications were significantly more prevalent in patients with diffuse CAD (Agatston score per vessel: 51 [IQR: 11-204] focal vs 158 [IQR: 52-341] diffuse;  $P = 0.024$ ). According to optical coherence tomography analysis, patients with focal CAD had a significantly higher prevalence of circumferential lipid-rich plaque ( $37\%$  focal vs  $4\%$  diffuse;  $P = 0.001$ ) and thin-cap fibroatheroma (TCFA) ( $47\%$  focal vs  $10\%$  diffuse;  $P = 0.002$ ). Focal disease defined by PPG predicted the presence of TCFA with an area under the curve of 0.73 (95% CI: 0.58-0.87).

**CONCLUSIONS** Atherosclerotic plaque phenotypes associate with intracoronary hemodynamics. Focal CAD had a higher plaque burden and was predominantly lipid-rich with a high prevalence of TCFA, whereas calcifications were more prevalent in diffuse CAD. (Precise Percutaneous Coronary Intervention Plan [P3]; [NCT03782688](https://clinicaltrials.gov/ct2/show/study/NCT03782688)) (J Am Coll Cardiol Img 2023;16:1452-1464) © 2023 The Authors. Published by Elsevier on behalf of the American College of Cardiology Foundation. This is an open access article under the CC BY-NC-ND license (<http://creativecommons.org/licenses/by-nc-nd/4.0/>).

From the <sup>a</sup>Cardiovascular Center Aalst, OLV Clinic, Aalst, Belgium; <sup>b</sup>Department of Medicine, Division of Cardiology, Showa University School of Medicine, Tokyo, Japan; <sup>c</sup>Division of Clinical Pharmacology, Department of Pharmacology, Showa University, Tokyo, Japan; <sup>d</sup>Department of Cardiovascular Medicine, Gifu Heart Center, Gifu, Japan; <sup>e</sup>Department of Medicine and Radiology, University of British Columbia, Vancouver, British Columbia, Canada; <sup>f</sup>Department of Cardiology, University of Milan, Milan, Italy; <sup>g</sup>Department of Advanced Biomedical Sciences, University Federico II, Naples, Italy; <sup>h</sup>Department of Cardiology, Aarhus University Hospital, Aarhus, Denmark; <sup>i</sup>Division of Cardiovascular Medicine, Department of Internal Medicine, Kobe University Graduate School of Medicine, Kobe, Japan; <sup>j</sup>Monash Cardiovascular Research Centre, Monash University and Monash Heart, Monash Health, Clayton, Victoria, Australia; <sup>k</sup>Department of Internal Medicine and Cardiovascular Center, Seoul National University Hospital, Seoul, South Korea; <sup>l</sup>Department of Internal Medicine, Discipline of

Coronary atherosclerosis can manifest as a broad range of plaque phenotypes.<sup>1</sup> Plaque differentiation and progression likely result from the interaction between multiple genetic and environmental factors, with the underlying inflammatory milieu playing an essential role.<sup>2-4</sup> Vessel hemodynamics, more specifically endothelial wall shear stress and tensile stress, have also been associated with specific plaque phenotypes.<sup>5,6</sup> However, the interplay between plaque morphology and local hemodynamics remains incompletely understood.<sup>7</sup>

Atherosclerosis can be characterized by using invasive and noninvasive imaging methods that quantify volume, extension, and composition. Large plaque burden and lipid-rich plaques (LRPs) have been identified as predictors of adverse clinical events.<sup>8-10</sup> Similarly, the presence of thin-cap fibroatheroma (TCFA) has been associated with plaque rupture, clinically manifested as acute myocardial infarction. Conversely, calcifications are considered markers of plaque stability.<sup>11</sup>

It has been postulated that the presence of focal pressure gradients may influence plaque biology and its propensity to rupture.<sup>12-14</sup> The pullback pressure gradient (PPG) is a quantitative index to quantify coronary artery disease (CAD) patterns into focal or diffuse CAD based on intravascular hemodynamics. Large-pressure gradients define focal disease, whereas the absence of focal gradients characterizes diffuse CAD.<sup>15</sup> We sought to investigate the pathophysiological interplay between physiological patterns and plaque characteristics using a combination of noninvasive and invasive imaging in patients with CAD.

## METHODS

**STUDY POPULATION.** The present study is a sub-analysis of the P3 (Precise Percutaneous Coronary Intervention Plan; NCT03782688) study. The main results have been published previously.<sup>16</sup> Briefly, this multicenter, prospective, single-arm study

was conducted in 5 countries. Patients with stable CAD and invasive fractional flow reserve (FFR)  $\leq 0.80$  were eligible for inclusion. All patients underwent coronary computed tomography angiography (CTA) with quantitative plaque analysis. Patients underwent an invasive procedure with motorized intracoronary pressure recordings for longitudinal vessel evaluation followed by optical coherence tomography (OCT). The P3 study validated a coronary CTA-based revascularization planning tool in predicting post-percutaneous coronary intervention (PCI) FFR. The objective of this substudy was to characterize atherosclerotic plaque phenotypes between focal and diffuse CAD defined by coronary hemodynamics using PPG.

The study protocol was approved by the investigational review board or ethics committee at each participating center. All patients signed informed consent before initiation of the study procedures.

**CORONARY CTA.** Coronary CTA was performed using the latest-generation CT scanners. Imaging acquisition guidelines recommended nitrates before CT acquisition and beta-blockers for heart rates  $>65$  beats/min. Calcium scores were calculated by the Agatston method at the vessel level. Absolute and relative plaque volumes were measured for each component.<sup>17,18</sup> Plaque burden was defined as plaque area divided by vessel area at the minimal lumen area (MLA). Percent atheroma volume (PAV) was defined as plaque volume divided by vessel volume.<sup>17</sup> Plaque composition was assessed by applying specific thresholds as described previously.<sup>19</sup> Low-attenuation plaque was defined as the presence of plaque with  $<30$  HU.<sup>20</sup> Positive remodeling was defined by a remodeling index  $>1.1$ .<sup>21,22</sup>

Coronary CTA images were analyzed by using validated software (QAngio CT, Medis Medical Imaging) by a core laboratory (CoreAalst BV) blinded to the invasive data.

## ABBREVIATIONS AND ACRONYMS

**CTA** = computed tomography angiography

**FFR** = fractional flow reserve

**LRP** = lipid-rich plaque

**MLA** = minimal lumen area

**OCT** = optical coherence tomography

**PAV** = percent atheroma volume

**PCI** = percutaneous coronary intervention

**PPG** = pullback pressure gradient

**TCFA** = thin-cap fibroatheromas

Cardiology, University of Campinas (Unicamp), Campinas, Brazil; <sup>m</sup>Centro Cardiologico Monzino, IRCCS, Milan, Italy; <sup>n</sup>Department of Biomedical and Clinical Sciences, University of Milan, Milan, Italy; <sup>o</sup>Department of Cardiology, Aichi Medical University, Aichi, Japan; <sup>p</sup>HeartFlow, Inc, Redwood City, California, USA; <sup>q</sup>Division of Cardiology, Department of Medicine, Weatherhead PET Center, McGovern Medical School, UTHealth and Memorial Hermann Hospital, Houston, Texas, USA; and the <sup>r</sup>Department of Cardiology, Lausanne University Hospital, Lausanne, Switzerland.

Jagat Narula, MD, served as Guest Editor for this paper.

The authors attest they are in compliance with human studies committees and animal welfare regulations of the authors' institutions and Food and Drug Administration guidelines, including patient consent where appropriate. For more information, visit the [Author Center](#).

**TABLE 1** Baseline Clinical Characteristics

	All (N = 117) <sup>a</sup>	Focal CAD (PPG >0.66) (n = 58)	Diffuse CAD (PPG ≤0.66) (n = 59)	P Value
Age, y	63.5 ± 9.3	61.9 ± 9.7	65.1 ± 8.7	0.062
Male	93 (79.5)	44 (75.9)	49 (83.1)	0.368
BMI, kg/m <sup>2</sup>	27.0 ± 3.4	26.9 ± 3.5	27.1 ± 3.3	0.771
Dyslipidemia	91 (77.8)	44 (75.9)	47 (79.7)	0.662
Hypertension	66 (56.4)	35 (60.3)	31 (52.5)	0.457
Diabetes mellitus	26 (22.2)	11 (19.0)	15 (25.4)	0.506
Smoking	24 (20.5)	13 (22.4)	11 (18.6)	0.653
Prior PCI	6 (5.1)	2 (3.4)	4 (6.8)	0.679
PAD	5 (4.3)	3 (5.2)	2 (3.4)	0.679
Stroke	4 (3.4)	3 (5.2)	1 (1.7)	0.364
Creatinine, mg/dL	0.94 ± 0.2	0.93 ± 0.22	0.95 ± 0.18	0.546
Creatinine clearance, mL/min	80.1 ± 23.9	83.9 ± 26.4	76.4 ± 20.6	0.097
LVEF, %	60.3 ± 6.2	60.4 ± 5.2	60.2 ± 7.0	0.826
Clinical presentation				0.041
Silent ischemia <sup>b</sup>	29 (24.8)	10 (17.2)	19 (32.2)	
CCS I	36 (30.8)	15 (25.9)	21 (35.6)	
CCS II	41 (35.0)	25 (43.1)	16 (27.1)	
CCS III	8 (6.8)	6 (10.3)	2 (3.4)	
CCS IV	1 (0.9)	0 (0.0)	1 (1.7)	
Unstable angina	2 (1.7)	2 (3.4)	0 (0.0)	
Agatston score per patient	230 (81-708)	147 (55-453)	462 (141-996)	0.025

Values are mean ± SD, n (%), or median (IQR), unless otherwise indicated. The lowest pullback pressure gradient (PPG) was used to classify the patients as having focal or diffuse coronary artery disease (CAD). <sup>a</sup>3 patients had 2 vessels assessed. <sup>b</sup>Silent ischemia is defined as asymptomatic patients with a positive noninvasive test result.

BMI = body mass index; CCS = Canadian Cardiovascular Society; LVEF = left ventricular ejection fraction; PAD = peripheral artery disease; PCI = percutaneous coronary intervention.

**INVASIVE PROCEDURE.** Invasive coronary angiography was performed following a dedicated protocol. Intracoronary nitroglycerin (100-200 µg) was administered before angiography. At least 2 projections separated by at least 30 degrees were obtained. Coronary angiography was analyzed with 3-dimensional quantitative coronary angiography (3D-QCA) software (CAAS 8.2 Software, Pie Medical Imaging). The location of the lesions was determined by measuring the distance between the ostium of the vessel and the MLA. Resting pressure ratios and FFR were measured in the distal segment of the vessel.

During intravenous adenosine infusion (140 µg/kg/min), FFR pullbacks at a speed of 1 mm/s were performed using a motorized device (R100, Volcano Corporation) fixed to the pressure wire.<sup>16</sup> From the FFR pullback curves, PPG was calculated using commercially available software (CoroFlow version

3.5, Coroventis Research AB). The PPG calculation has been described in detail elsewhere.<sup>15</sup> Briefly, PPG combines 2 parameters extracted from FFR pullback curves: first, the maximal pressure gradient over 20% of the pullback, and second, the length of functional disease. PPG ranges from 0 (diffuse disease) to 1 (focal disease). For the present analysis, the median PPG value dichotomized focal vs diffuse CAD. Aortic pressure tracings without a dirotic notch, ventricularization, drift >0.05 FFR unit, unstable hyperemic conditions during the pullback maneuver, and pullback curves with major artifacts were excluded.

Optical coherence tomography (OCT) pullbacks of 75 mm were acquired using a Dragonfly OPTIS Imaging Catheter (Abbott Vascular). An automated algorithm defined MLA. OCT pullbacks were performed before balloon predilatation when feasible; cases in which OCT was performed after predilatation were excluded from the OCT plaque analysis. LRP were defined as a low-signal region with a diffuse border of at least 90 degrees with a length >1 mm.<sup>23</sup> Circumferential LRP was defined as lipid occupying 360 degrees. A fibrous cap was defined as a signal-rich homogeneous layer overlying an LRP.<sup>24</sup> The thinnest part of the fibrous cap was measured 3 times, and its average thickness was defined as the fibrous cap thickness. TCFA was defined as the presence of fibrous cap thickness <65 µm overlying LRP.<sup>25</sup> Plaque rupture was defined as intimal tearing, disruption, or dissection of the cap. Additional OCT definitions are shown in Supplemental Table 1.<sup>26,27</sup> OCT images were analyzed by the core laboratory using CAAS Intravascular version 2.1 (Pie Medical Imaging) blinded to the physiological data.

**STATISTICAL ANALYSIS.** Variables are expressed as mean ± SD and median (IQR) for normally and non-normally distributed data, respectively. Categorical variables are expressed as frequencies and percentages. Continuous variables were compared by using the Student's *t*-test (or Mann-Whitney tests as appropriate), and categorical variables were compared by using the chi-square (or the Fisher exact test as appropriate). The Pearson correlation coefficient was used to assess the relationship between continuous variables. Univariable and multivariable regression analyses with logistic and generalized linear models were used to assess the association between CAD patterns defined by PPG (predictor variable) and plaque characteristics derived from coronary CTA and OCT (outcome variables). PPG and

FFR were analyzed as continuous variables. Receiver-operating characteristic curve analyses were used to assess the capacity of PPG to predict adverse plaque characteristics. In patients with multivessel interrogation (n = 3), the lowest PPG value was used to classify the case for the patient-level analysis.

A value of  $P \leq 0.05$  was considered to indicate statistical significance. All statistical analyses were performed by using R version 4.1.2 (R Foundation for Statistical Computing).

**RESULTS**

**STUDY POPULATION.** From February 2019 to December 2020, a total of 259 patients were screened, and 117 patients (120 vessels) were included. The study flowchart is shown in [Supplemental Figure 1](#). Coronary CTA plaque analysis was feasible for all cases, and OCT plaque analysis was feasible in 57% (68 of 120) of the cases.

**BASELINE CHARACTERISTICS.** Clinical characteristics stratified according to CAD pattern are shown in [Table 1](#). Mean age tended to be lower in patients with focal CAD, most of the patients were male, and one-fifth had diabetes, all without differences between focal and diffuse disease. Procedural, morphologic, and coronary physiology characteristics stratified according to CAD patterns are shown in [Table 2](#). Diffuse CAD was more frequently observed in the left anterior descending artery. The median PPG was 0.66 (IQR: 0.54-0.75). PPG distribution and its relationship with lesion severity are shown in [Figure 1](#). Patients with focal vs diffuse disease CAD had greater lesion severity, represented by smaller MLA in 3D-QCA and lower FFR. A sensitivity analysis restricted to patients with single-vessel interrogation is shown in [Supplemental Table 2](#).

**PLAQUE MORPHOLOGY BASED ON CORONARY CTA STRATIFIED ACCORDING TO CAD PATTERN.** The mean plaque burden (at the MLA) was  $85\% \pm 9\%$  and was significantly higher in patients with focal CAD. Conversely, PAV (vessel level) was higher in patients with diffuse CAD. Patients with diffuse CAD had a higher Agatston score, longer calcium length, and higher calcified plaque burden than those with focal CAD ([Table 3](#), [Figure 2](#)). Other plaque components based on coronary CTA stratified according to the PPG are shown in [Supplemental Table 3](#).

FFR was associated with plaque burden at the MLA ([Supplemental Table 4](#)). PPG was significantly associated with plaque burden at the MLA, noncalcified

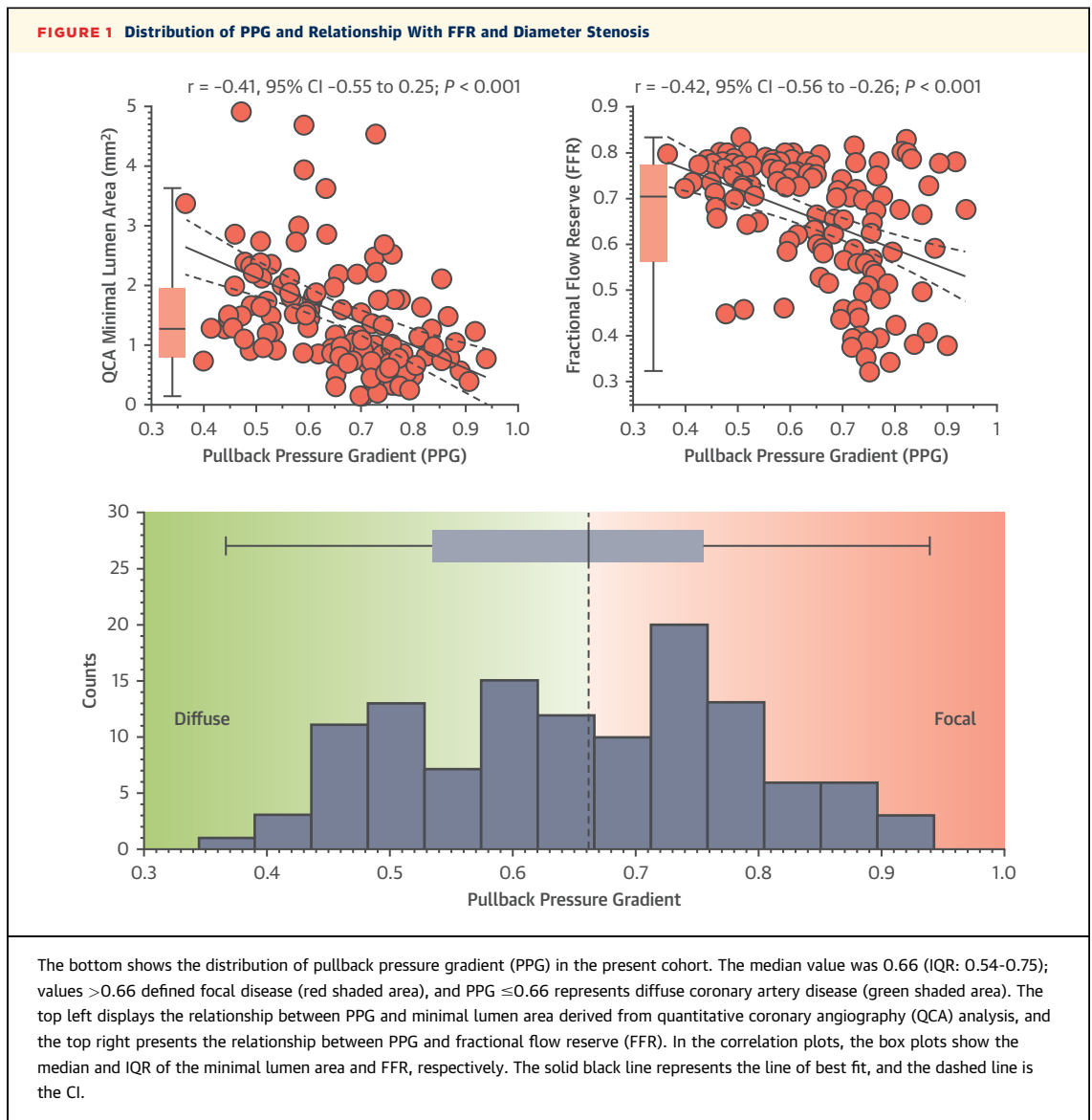
**TABLE 2 Imaging and Hemodynamic Vessel Characteristics**

	All (N = 120)	Focal CAD (PPG >0.66) (n = 60)	Diffuse CAD (PPG ≤0.66) (n = 60)	P Value
Vessels				<0.001
LAD	92 (76.7)	35 (58.3)	57 (95.0)	
LCx	13 (10.8)	11 (18.3)	2 (3.3)	
RCA	15 (12.5)	14 (23.3)	1 (1.7)	
QCA analysis				
Minimum lumen diameter, mm	1.3 ± 0.43	1.1 ± 0.38	1.5 ± 0.40	<0.001
Reference lumen diameter, mm	2.7 ± 0.49	2.7 ± 0.49	2.7 ± 0.49	0.959
Diameter stenosis, %	51.6 ± 14.0	58.8 ± 11.4	44.5 ± 12.8	<0.001
Area stenosis, %	74.7 ± 14.4	81.9 ± 10.2	67.5 ± 14.6	<0.001
Location of the lesion, mm <sup>a</sup>	40.6 ± 18.0	40.1 ± 19.5	41.0 ± 16.4	0.789
OCT analysis				
Number of vessels	68	19 <sup>b</sup>	49 <sup>c</sup>	
Lesion length, mm	29.8 ± 12.9	26.8 ± 11.5	31.0 ± 13.4	0.23
Minimum lumen area, mm <sup>2</sup>	1.8 ± 0.76	1.4 ± 0.71	2.0 ± 0.74	0.007
Area stenosis, %	73.2 ± 11.1	83.7 ± 3.5	69.2 ± 10.4	<0.001
Physiological analysis				
Resting Pd/Pa	0.82 ± 0.14	0.77 ± 0.17	0.88 ± 0.06	<0.001
FFR	0.65 ± 0.14	0.59 ± 0.15	0.72 ± 0.09	<0.001
PPG	0.66 ± 0.13	0.77 ± 0.07	0.54 ± 0.08	<0.001

Values are n (%) or mean ± SD, unless otherwise indicated. <sup>a</sup>Distance between the ostium and minimal lumen area assessed using quantitative coronary angiography. <sup>b</sup>41 vessels were excluded because predilatation was performed before optical coherence tomography (OCT) acquisition to facilitate catheter advancement. <sup>c</sup>11 vessels were excluded because predilatation was performed before OCT acquisition to facilitate catheter advancement.  
 FFR = fractional flow reserve; LAD = left anterior descending; LCx = left circumflex; Pa = aortic pressure; Pd = distal coronary pressure; QCA = quantitative coronary angiography; RCA = right coronary artery; other abbreviations as in [Table 1](#).

and calcified plaque burdens, low-attenuation plaque burden, PAV, and Agatston score ([Table 4](#)); the higher the PPG, the larger the plaque burden at the MLA, the greater the low-attenuation plaque and noncalcified plaque and the lower the calcified plaque burden. PPG remained associated with plaque coronary CTA characteristics independent of FFR ([Supplemental Table 5](#)).

**PLAQUE MORPHOLOGY BASED ON OCT STRATIFIED ACCORDING TO CAD PATTERNS.** LRP were present in 57% of cases, and circumferential LRP was significantly more prevalent in patients with focal CAD. Associations between PPG and OCT plaque features are presented in [Table 4](#) and [Figure 3](#). PPG predicted the presence of circumferential LRP with an area under the curve of 0.82 (95% CI: 0.66-0.99). In vessels with focal CAD, fibrous caps overlying fibroatheromas were thinner ( $63 \pm 9.9 \mu\text{m}$  focal vs  $90.3 \pm 25.2 \mu\text{m}$  diffuse;  $P = 0.001$ ) and TCFA more prevalent (47.4% focal vs 10.2% diffuse;  $P = 0.002$ ) than in vessels with diffuse disease. PPG and fibrous cap thickness were negatively correlated ( $r = -0.55$  [95% CI: -0.74 to



-0.28];  $P < 0.001$ ). PPG was associated with fibrous cap thickness independent of FFR and diabetes mellitus (Supplemental Table 6). High PPG predicted the presence of TCFA with an area under the curve of 0.73 (95% CI: 0.58-0.87). Independent of FFR, PPG was significantly associated with the presence of circumferential LRP, TCFA, and plaque rupture (Supplemental Table 7). FFR was not associated with OCT plaque characteristics (Supplemental Table 8). Two case examples summarizing the association between plaque characteristics according to coronary CTA and OCT and coronary physiology are shown in Figure 4. The Central Illustration summarizes the

association between pathophysiology patterns of CAD defined according to PPG and plaque characteristics based on invasive and noninvasive imaging.

## DISCUSSION

The present study describes the interplay between coronary hemodynamics and atherosclerotic plaque phenotypes. The main finding is the distinctive plaque features observed in patients with focal vs diffuse CAD. Atherosclerotic lesions in vessels with focal disease (high PPG) had a higher plaque burden and were predominantly lipid-rich with a high prevalence

of TCFA, whereas calcifications were the hallmark of vessels with diffuse disease (low PPG). Furthermore, translesion pressure gradients correlated inversely with fibrous cap thickness.

Previous studies have shown that low FFR, measured at the distal segment of the coronary artery, is associated with plaque characteristics, particularly the presence of plaques at higher risk of rupture.<sup>12,28</sup> However, these studies are limited by the absence of longitudinal vessel hemodynamic information. PPG, derived from hyperemic pullback pressure curves, quantifies the longitudinal distribution of epicardial resistance, thus providing a second dimension to single-point FFR.<sup>29</sup> A unique feature of our methodology is the use of motorized pullback recordings, which increased the accuracy of the analysis and allowed for the standardization of the pressure-length relationship.<sup>30</sup> Translesion pressure gradients concentrated on a short segment of the artery (ie, high PPG) translate into increased plaque tensile and compressive stresses.<sup>31</sup> Focal disease, defined by coronary physiology with PPG, was anatomically more severe and had a greater plaque burden, explaining the lower FFR measured at the distal coronary segment than vessels with diffuse disease. These localized pressure gradients also induce disturbance of laminar flow with eddies at the lesion exit, producing areas of low and oscillatory wall shear stress, which can lead to plaque progression and inflammation, cap thinning and destabilization, and, ultimately, plaque rupture when the physical forces exerted on the plaque exceed its material strength.<sup>31,32</sup>

In the present study, we observed that high PPG values were associated with plaque rupture and a negative relationship between PPG and cap thickness overlying fibroatheromas. In contrast, in vessels with a low PPG value, epicardial resistance was spread over a longer vessel segment. These findings expand our knowledge about the relationship between coronary physiology, quantified by FFR and PPG, and plaque characteristics assessed invasively using OCT and noninvasively through coronary CTA.

It can be hypothesized that lipidic plaque progression occurs rapidly, with localized growth leading to focal stenosis, here captured as high PPG. Conversely, in the absence of focal pressure gradients, the prevalence of LRPs was low, and low PPG values were mainly associated with coronary calcifications. Patients with diffuse pressure losses had higher calcium scores, calcium burden, and calcium volume derived from the quantitative coronary CTA

**TABLE 3** Plaque Characteristics Based on Coronary CTA and OCT in Focal and Diffuse CAD

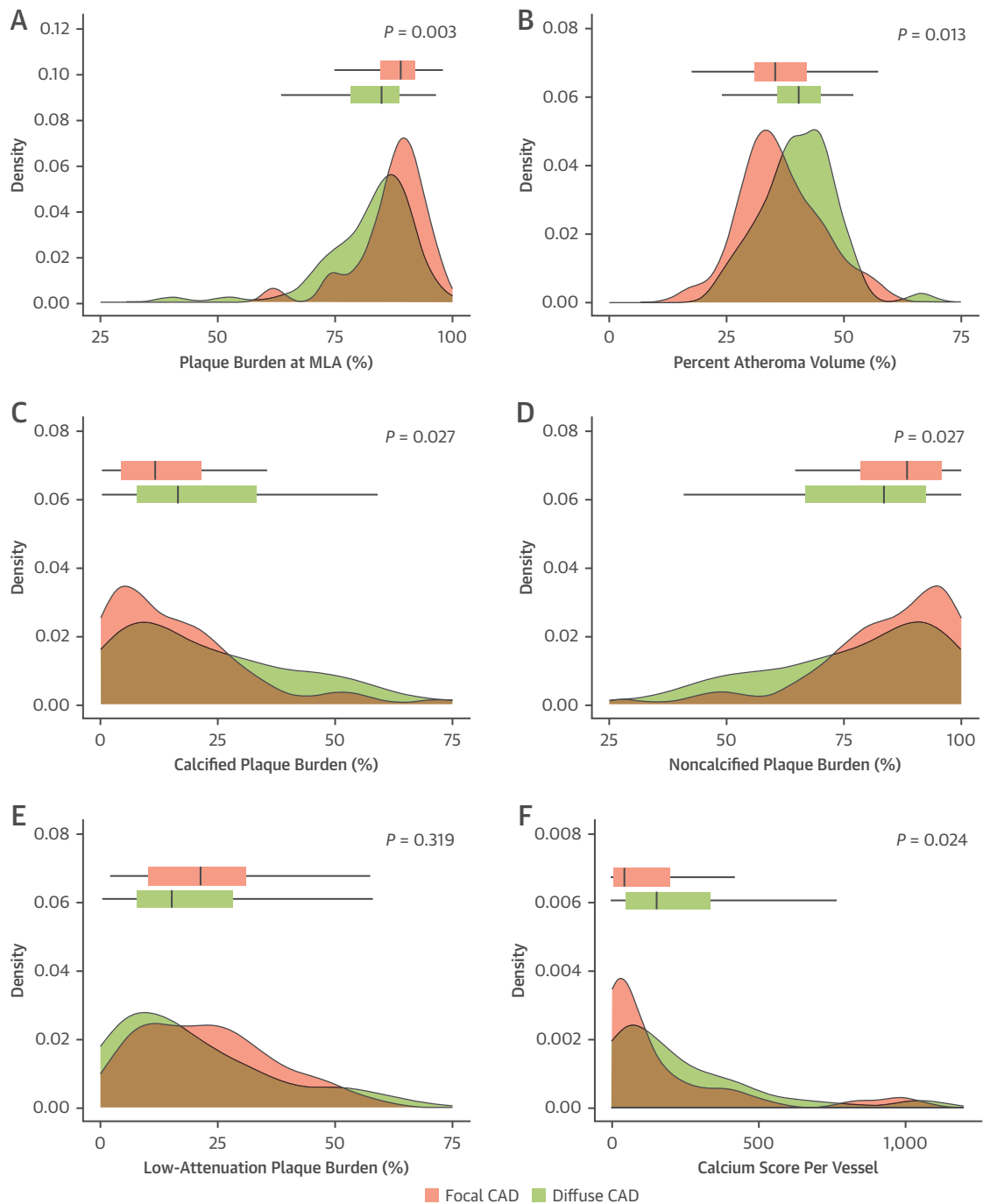
	All	Focal CAD (PPG >0.66)	Diffuse CAD (PPG ≤0.66)	P Value
<b>Coronary CTA plaque analysis</b>				
Number of vessels	120	60	60	
<b>Lesion level</b>				
Plaque burden at the MLA, %	84.7 ± 9.0	87.1 ± 7.5	82.3 ± 9.8	0.003
Remodeling index	0.93 ± 0.21	0.94 ± 0.19	0.93 ± 0.23	0.760
Noncalcified plaque burden, %	80.9 ± 17.0	84.4 ± 14.9	77.5 ± 18.3	0.027
Low-attenuation plaque burden, %	21.3 ± 15.4	22.7 ± 14.0	19.9 ± 16.7	0.319
Napkin-ring sign	7 (5.8)	4 (6.7)	3 (5.0)	1.0
Calcified plaque burden, %	19.1 ± 17.0	15.7 ± 14.9	22.5 ± 18.3	0.027
Calcium length, mm	6.0 ± 6.5	4.1 ± 5.6	7.7 ± 6.8	0.011
Calcium arc, degrees	45 (0-150)	0 (0-90)	55 (30-180)	0.022
Spotty calcification	30 (25.0)	19 (31.7)	11 (18.3)	0.139
<b>Vessel level analysis</b>				
Atheroma volume, %	38.5 ± 8.3	36.6 ± 8.5	40.3 ± 7.8	0.013
Noncalcified plaque burden, %	84.7 ± 13.7	86.5 ± 12.7	82.8 ± 14.4	0.147
Low-attenuation plaque burden, %	18.0 ± 12.1	17.9 ± 11.0	18.2 ± 13.1	0.888
Agatston score per vessel	104 (31-300)	51 (11-204)	158 (52-341)	0.024
<b>OCT plaque analysis</b>				
Number of vessels	68	19	49	
LRP	39 (57.4)	14 (73.7)	25 (51.0)	0.108
LRP >180 degrees	30 (44.1)	12 (63.2)	18 (36.7)	0.061
Circumferential LRP	9 (13.2)	7 (36.8)	2 (4.1)	0.001
Calcified plaque	55 (80.9)	13 (68.4)	42 (85.7)	0.166
Eruptive calcified nodule	3 (4.4)	0 (0.0)	3 (6.1)	0.554
Spotty calcium	16 (23.5)	3 (15.8)	13 (26.5)	0.526
Thin-cap fibroatheroma	14 (20.6)	9 (47.4)	5 (10.2)	0.002
Plaque rupture	18 (26.5)	7 (36.8)	11 (22.4)	0.238
Thrombus	13 (19.1)	6 (31.6)	7 (14.3)	0.166
Micro channel	25 (36.8)	6 (31.6)	19 (38.8)	0.780
Macrophage accumulation	18 (26.5)	5 (26.3)	13 (26.5)	1.000
Cholesterol crystal	22 (32.4)	7 (36.8)	15 (30.6)	0.773
Layered plaque	44 (64.7)	14 (73.7)	30 (61.2)	0.405
Values are mean ± SD, n (%), or median (IQR) unless otherwise indicated. CTA = computed tomography angiography; LRP = lipid-rich plaque; MLA = minimal lumen area; other abbreviations as in Tables 1 and 2.				

analysis. Plaque calcification stabilizes CAD by decreasing fibrous cap stress.<sup>11</sup> Moreover, calcifications influence coronary artery interventions and are associated with fewer procedural successes and a higher rate of long-term complications after PCI.<sup>33</sup> Interestingly, the PAV was greater in diffuse disease. PAV and calcifications are also considered prognostic indicators, but instead of identifying plaque-related risk, they reflect the general burden of disease.

TCFA can be observed in a broad range of angiographic lesion severity; however, they are twice as common in severe stenosis than in nonsevere stenosis.<sup>34</sup> This finding is compatible with the present study, in which patients with focal disease (high PPG) had lower FFR and more TCFA. This is also consistent



**FIGURE 2** Plaque Characteristics Based on Coronary CTA in Focal and Diffuse Disease



The box plots show coronary computed tomography angiography (CTA)-derived plaque characteristics stratified according to coronary artery disease pattern. Focal coronary artery disease is depicted in red, and diffuse disease is in green. (A) Plaque burden at the minimal lumen area (MLA). (B) Percent atheroma volume (vessel level). (C) Calcified plaque burden. (D) Noncalcified plaque burden. (E) Low-attenuation plaque burden. (F) Agatston score per vessel.

with the observation that acute coronary syndrome occur more frequently in cases with significant stenosis.<sup>35</sup> Interestingly, the association between PPG and TCFA was independent of FFR, highlighting the role of local hemodynamics on plaque characteristics. The presence of lipidic plaque and TCFA has been shown to predict the occurrence of ischemic events; however, the limited predictive capacity of adverse events using these plaques impedes their use for revascularization decisions. A prospective natural history study of coronary atherosclerosis with novel imaging and physiological techniques is warranted.

The PPG will allow for connecting coronary physiology patterns with plaque characteristics. Because the PPG is easily obtainable in practice after a manual 20- to 30-second FFR pullback maneuver, the present findings have several clinical implications. Beyond the classical evaluation of lesion significance with FFR, a pullback maneuver not only adds additional information on the likelihood of PCI success but also provides further stratification on patients' risk for adverse events.<sup>36</sup> High PPG predicted the presence of circumferential LRPs and TCFA with an area under the curve of 0.82 and 0.73, respectively. This atherosclerotic phenotyping based on coronary physiology allows for the understanding of CAD as 2 entities: focal disease, with a predominantly lipidic atherosclerotic pattern, and diffuse disease, with a more stable atherosclerotic and hemodynamic pattern. Clinically, focal disease is more amenable to therapies such as PCI, and based on the linked lipidic plaque phenotype, this patient subgroup benefits from an intervention.<sup>37,38</sup> In contrast, diffuse disease, less appropriate for PCI and stable in nature, may benefit more from conservative management. The PPG may facilitate standardization of the diagnosis of CAD patterns and be able to identify individuals with different responses to coronary interventions. A randomized clinical trial addressing the clinical benefit of a PPG-guided treatment strategy is required.

**STUDY LIMITATIONS.** The main limitation of the present study is that it represents a snapshot of the atherosclerosis process. Because of the lack of serial data, we could not assess disease progression or the clinical outcomes associated with focal and diffuse disease. In addition, OCT was not available for all patients, with a higher image attrition rate in patients with focal CAD, mainly because of technical difficulties during image acquisition. Nonetheless, this was partly circumvented by the coronary CTA analysis available in the complete cohort. Furthermore,

**TABLE 4 Univariable Regression Analysis of PPG for the Association of Plaque Characteristics Based on Coronary CTA and OCT**

	Beta	95% CI	P Value
<b>Coronary CTA plaque analysis<sup>a</sup></b>			
Plaque burden at MLA	2.06	0.90 to 3.23	<0.001
Remodeling index	0.01	-0.02 to 0.04	0.558
Noncalcified plaque burden (lesion level)	3.60	1.39 to 5.82	0.002
Low-attenuation plaque burden (lesion level)	2.27	0.22 to 4.33	0.032
Calcified plaque burden (lesion level)	-3.60	-5.82 to -1.39	0.002
Percent atheroma volume (vessel level)	-1.80	-2.88 to -0.71	0.002
Agatston score per vessel (vessel level)	-55.38	-105.63 to -5.13	0.034
	Odds Ratio	95% CI	P Value
<b>OCT plaque analysis<sup>b</sup></b>			
LRP >180°	1.72	1.14 to 2.71	0.013
Circumferential LRP	3.01	1.57 to 6.93	0.003
Thin-cap fibroatheroma	1.83	1.13 to 3.15	0.018
Plaque rupture	1.61	1.04 to 2.58	0.040
Eruptive calcified nodule	0.80	0.25 to 2.03	0.657
Spotty calcium	0.73	0.44 to 1.17	0.212
Microchannels	1.08	0.73 to 1.62	0.688
Macrophage accumulation	1.06	0.68 to 1.63	0.806
Cholesterol crystals	1.10	0.73 to 1.65	0.660
Layered plaque	1.30	0.86 to 2.01	0.224

The explanatory variable was the PPG as a continuous variable. <sup>a</sup>Continuous variables. <sup>b</sup>Categorical variables. Abbreviations as in Tables 1 to 3.

information on microcirculation, which has been associated with plaque characteristics, was not collected.<sup>7</sup> Moreover, we acknowledge that despite adjusting the association between plaque features and PPG by FFR, the absence of vessels with high FFR (FFR >0.80) may have influenced the analysis. It is important to highlight that the patients included in this study had hemodynamically significant lesions defined as FFR ≤0.80. The extrapolation of these findings to patients with hemodynamically nonsignificant lesions requires further investigation. Finally, the present study was focused on the association between coronary hemodynamics and plaque characteristics; the impact of these findings on clinical outcomes remains to be determined.

**CONCLUSIONS**

Atherosclerotic plaque phenotypes associate with intracoronary hemodynamics. Vessels with focal disease (high PPG) had a higher plaque burden and predominantly LRPs with a high prevalence of TCFA, whereas in vessels with diffuse disease (low PPG), the plaques were predominantly calcified. PPG was associated with cap thickness, with thinner caps



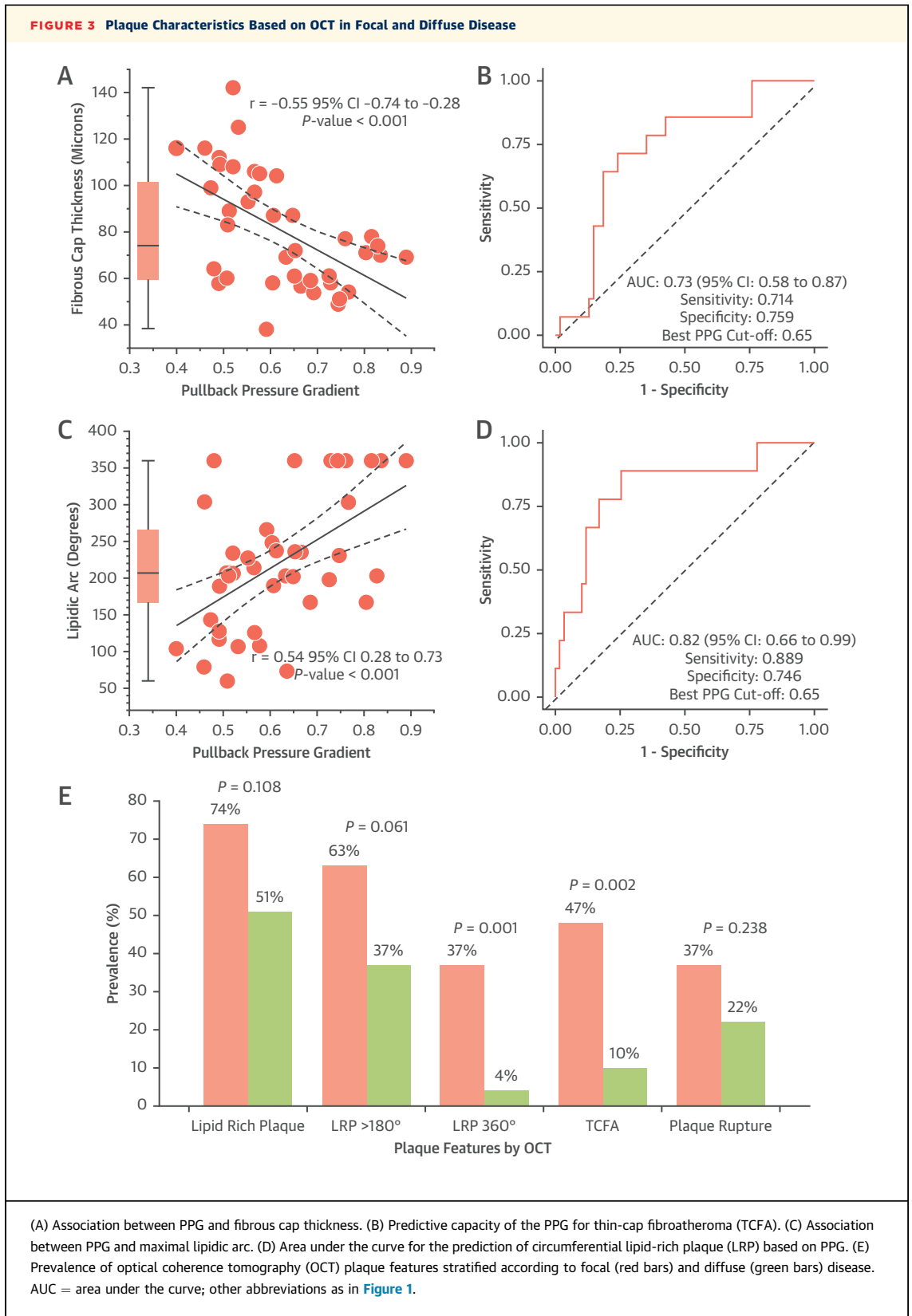
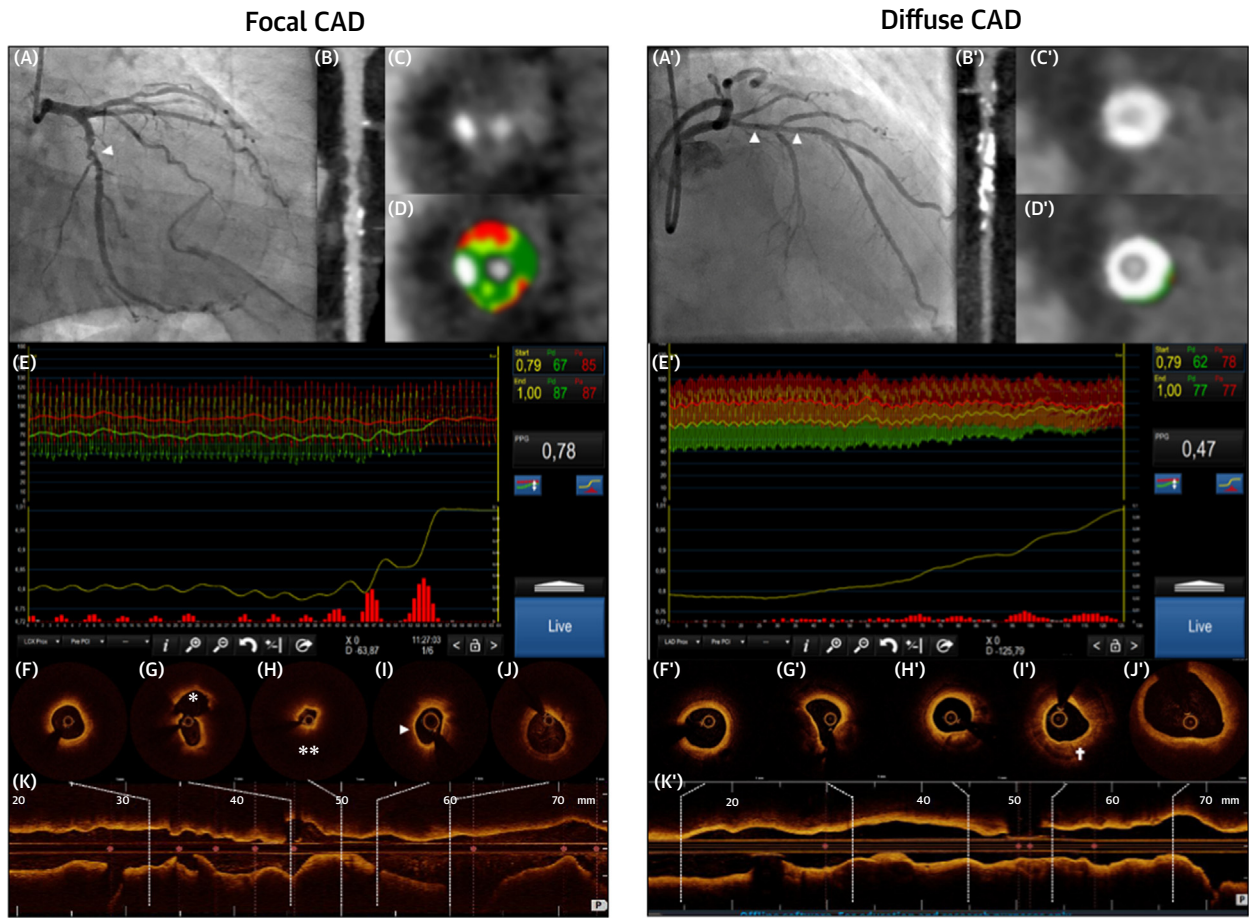


**FIGURE 4** Case Examples of Focal and Diffuse CAD



The left shows a case with focal coronary artery disease (CAD) (high PPG), whereas the right shows a patient with diffuse CAD. A and A' indicate coronary angiography, and the white arrowheads identify the lesions. B and B' indicate coronary CTA straight multiplanar reconstructions of the vessel, and C and C' and D and D' show the cross-section without and with tissue characterization, respectively. E and E' present the FFR pullback tracings with the corresponding FFR and PPG values. The red bars depict the location and magnitude of pressure drops along the coronary vessel. F to K show cross-sectional and longitudinal optical coherence tomography images, respectively. The asterisk indicates plaque rupture, 2 asterisks depict circumferential lipid-rich plaque, the arrowhead indicates thin-cap fibroatheroma, and the white dagger indicates circumferential calcified plaque. Abbreviations as in [Figures 1 and 2](#).

observed in lesions with higher focal pressure gradients.

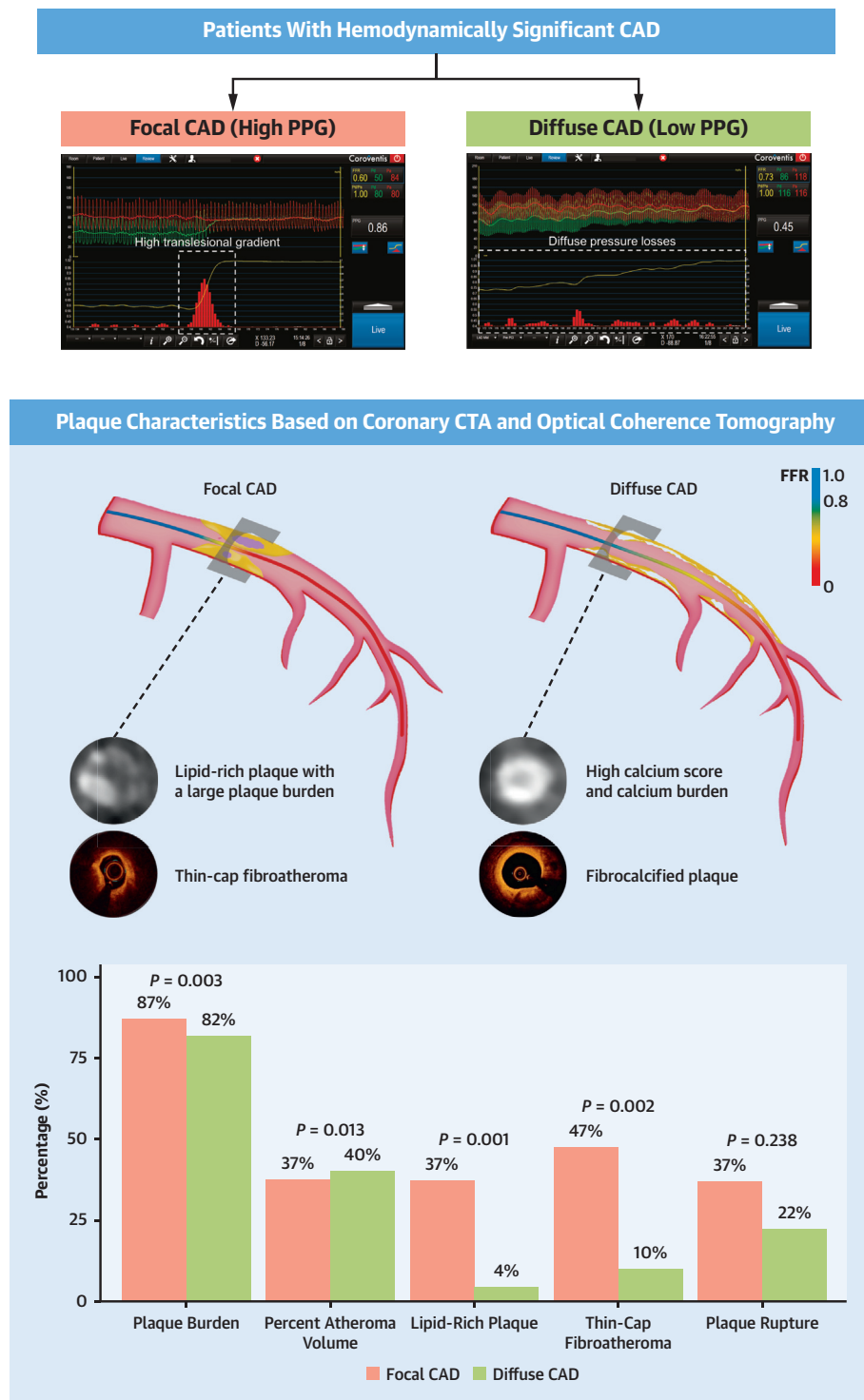
These results relate invasive pathophysiology and plaque characteristics supporting the clinical utility of FFR and PPG for differentiating focal from diffuse disease. The data support the use and interpretation of PPG in relation to plaque composition but do not support the use of anatomic plaque characteristics by either coronary CTA or OCT as a basis for revascularization in the absence of reduced FFR. In addition, the absence of comparable plaque evaluation for nonhemodynamically significant lesions (FFR >0.80) precludes extrapolating these findings to a less diseased population.

**ACKNOWLEDGMENT** The authors appreciate the support of the co-investigators and study coordinators participating in the P3 study.

#### FUNDING AND AUTHOR DISCLOSURES

The study was sponsored by the Cardiac Research Institute Aalst with unrestricted grants from HeartFlow Inc. Dr Mizukami has received consulting fees from Zeon Medical and HeartFlow Inc; and speaker fees from Abbott Vascular. Dr Leipsic is a consultant and has holding stock options in Circle CVI and HeartFlow Inc; has received a research grant from GE; and modest speaker fees from GE and Philips. Drs Sonck and Munhoz have received research grants provided by the Cardiopath Ph.D. program. Dr Nørgaard has received unrestricted institutional research grants from Siemens and HeartFlow Inc. Dr Otake has received research grants from Abbott Vascular; and speaker

**CENTRAL ILLUSTRATION Association Between CAD Patterns and Plaque Characteristics Based on Invasive and Noninvasive Imaging**



Sakai K, et al. J Am Coll Cardiol Img. 2023;16(11):1452-1464.

The study included patients with hemodynamically significant coronary artery disease (CAD) based on fractional flow reserve (FFR)  $\leq 0.80$  with plaque characterization based on coronary computed tomography angiography (CTA) and optical coherence tomography. Based on the pullback pressure gradient (PPG) index, patients were divided into those with focal (PPG  $> 0.66$ ) or diffuse (PPG  $\leq 0.66$ ) CAD. Vessels with focal CAD (red bars) had a higher plaque burden and predominantly lipid-rich plaque with a high prevalence of thin-cap fibroatheroma, whereas calcifications were the hallmark of vessels with diffuse disease (green bars).

fees from HeartFlow Inc and Abbott Vascular. Dr Ko has received consulting fees from Canon Medical, Abbott, and Medtronic. Dr Koo has received institutional research grants from HeartFlow Inc. Dr Maeng has received advisory board and lecture fees from AstraZeneca, Bayer, Boehringer Ingelheim, Bristol Myers Squibb, Boston Scientific, and Novo Nordisk; and research grants from Bayer and Philips Healthcare. Dr Jensen has received unrestricted institutional research grants from Siemens and HeartFlow Inc. Dr Andreini has received research grants from GE Healthcare and Bracco. Dr Shinke has received research grants from Boston Scientific and Abbott Vascular. CT is an employee of HeartFlow Inc. Dr Barbato has received speaker fees from Boston Scientific, Abbott Vascular, and GE. Dr Johnson has received internal funding from the Weatherhead PET Center for Preventing and Reversing Atherosclerosis; significant institutional research support from St. Jude Medical (CONTRAST [Can Contrast Injection Better Approximate FFR Compared to Pure Resting Physiology?]); NCT02184117 and Philips/Volcano Corporation (DEFINE-FLOW [Combined Pressure and Flow Measurements to Guide Treatment of Coronary Stenoses]; NCT02328820) for studies using intracoronary pressure and flow sensors; has an institutional licensing agreement with Boston Scientific for the smart-minimum FFR algorithm commercialized under 510(k) K191008; and has pending patents on diagnostic methods for quantifying aortic stenosis and transcatheter aortic valve replacement physiology, as well as algorithms to correct pressure tracings from fluid-filled catheters. Dr De Bruyne has received consultancy fees from Boston Scientific and Abbott Vascular; research grants from Coroventis Research, Pie Medical Imaging, CathWorks, Boston Scientific, Siemens, HeartFlow Inc, and Abbott Vascular; and owns equity in Siemens, GE, Philips, HeartFlow Inc, Edwards Life Sciences, Bayer, Sanofi, and Celyad. Dr Collet has received research grants from Biosensor, Coroventis Research, Medis Medical Imaging, Pie Medical Imaging, CathWorks,

Boston Scientific, Siemens, HeartFlow Inc, and Abbott Vascular; and consultancy fees from HeartFlow Inc, OpSens, Abbott Vascular, and Philips Volcano. All other authors have reported that they have no relationships relevant to the contents of this paper to disclose.

**ADDRESS FOR CORRESPONDENCE:** Dr Carlos Collet, Cardiovascular Center, Onze-Lieve-Vrouwziekenhuis, Moorselbaan 164, Aalst 9300, Belgium. E-mail: carloscollet@gmail.com.

## PERSPECTIVES

### COMPETENCY IN PATIENT CARE AND PROCEDURAL

**SKILLS:** In patients with stable CAD, focal hemodynamic disease correlates with plaque morphology. Focal disease is associated with LRPs with a high prevalence of TCFA, whereas diffuse disease relates to calcified plaque. These data suggest that patient risk can be stratified according to coronary physiology.

**TRANSLATIONAL OUTLOOK:** The PPG segregates CAD into 2 phenotypes with different associated risks. Prospective studies are needed to establish the clinical benefit of a PPG-guided treatment strategy with revascularization of focal lesions and conservative management of the diffuse disease.

## REFERENCES

1. Libby P. The changing landscape of atherosclerosis. *Nature*. 2021;592:524-533.
2. Aherrahrou R, Guo L, Nagraj VP, et al. Genetic regulation of atherosclerosis-relevant phenotypes in human vascular smooth muscle cells. *Circ Res*. 2020;127:1552-1565.
3. Geovanani GR, Libby P. Atherosclerosis and inflammation: overview and updates. *Clin Sci (Lond)*. 2018;132:1243-1252.
4. Wolf D, Ley K. Immunity and inflammation in atherosclerosis. *Circ Res*. 2019;124:315-327.
5. Wentzel JJ, Janssen E, Vos J, et al. Extension of increased atherosclerotic wall thickness into high shear stress regions is associated with loss of compensatory remodeling. *Circulation*. 2003;108:17-23.
6. Kwak BR, Back M, Bochaton-Piallat ML, et al. Biomechanical factors in atherosclerosis: mechanisms and clinical implications. *Eur Heart J*. 2014;35:3013-3020, 3020a-3020d.
7. Yang S, Koo BK, Narula J. Interactions between morphological plaque characteristics and coronary physiology: from pathophysiological basis to clinical implications. *J Am Coll Cardiol Img*. 2022;15:1139-1151.
8. Stone GW, Maehara A, Lansky AJ, et al. A prospective natural-history study of coronary atherosclerosis. *N Engl J Med*. 2011;364:226-235.
9. Prati F, Romagnoli E, Gatto L, et al. Relationship between coronary plaque morphology of the left anterior descending artery and 12 months clinical outcome: the CLIMA study. *Eur Heart J*. 2020;41:383-391.
10. Waksman R, Di Mario C, Torguson R, et al. Identification of patients and plaques vulnerable to future coronary events with near-infrared spectroscopy intravascular ultrasound imaging: a prospective, cohort study. *Lancet*. 2019;394:1629-1637.
11. Huang H, Virmani R, Younis H, Burke AP, Kamm RD, Lee RT. The impact of calcification on the biomechanical stability of atherosclerotic plaques. *Circulation*. 2001;103:1051-1056.
12. Matsuo Y, Higashioka D, Ino Y, et al. Association of hemodynamic severity with plaque vulnerability and complexity of coronary artery stenosis: a combined optical coherence tomography and fractional flow reserve study. *J Am Coll Cardiol Img*. 2019;12:1103-1105.
13. Lee JM, Choi G, Koo BK, et al. Identification of high-risk plaques destined to cause acute coronary syndrome using coronary computed tomographic angiography and computational fluid dynamics. *J Am Coll Cardiol Img*. 2019;12:1032-1043.
14. Pagnoni M, Meier D, Candrea A, et al. Future culprit detection based on angiography-derived FFR. *Catheter Cardiovasc Interv*. 2021;98:E388-E394.
15. Collet C, Sonck J, Vandeloos B, et al. Measurement of hyperemic pullback pressure gradients to characterize patterns of coronary atherosclerosis. *J Am Coll Cardiol*. 2019;74:1772-1784.
16. Sonck J, Nagumo S, Norgaard Bjarne L, et al. Clinical validation of a virtual planner for coronary interventions based on coronary CT angiography. *J Am Coll Cardiol Img*. 2022;15:1242-1255.
17. Williams MC, Kwiecinski J, Doris M, et al. Low-attenuation noncalcified plaque on coronary computed tomography angiography predicts myocardial infarction: results from the multicenter SCOT-HEART Trial (Scottish Computed Tomography of the HEART). *Circulation*. 2020;141:1452-1462.
18. Monizzi G, Sonck J, Nagumo S, et al. Quantification of calcium burden by coronary CT angiography compared to optical coherence tomography. *Int J Cardiovasc Imaging*. 2020;36:2393-2402.
19. Matsumoto H, Watanabe S, Kyo E, et al. Standardized volumetric plaque quantification and

- characterization from coronary CT angiography: a head-to-head comparison with invasive intravascular ultrasound. *Eur Radiol*. 2019;29:6129–6139.
20. Dey D, Diaz Zamudio M, Schuhbaeck A, et al. Relationship between quantitative adverse plaque features from coronary computed tomography angiography and downstream impaired myocardial flow reserve by <sup>13</sup>N-ammonia positron emission tomography: a pilot study. *Circ Cardiovasc Imaging*. 2015;8:e003255.
  21. Achenbach S, Ropers D, Hoffmann U, et al. Assessment of coronary remodeling in stenotic and nonstenotic coronary atherosclerotic lesions by multidetector spiral computed tomography. *J Am Coll Cardiol*. 2004;43:842–847.
  22. Park H-B, Heo R, Hartaigh BÓ, et al. Atherosclerotic plaque characteristics by CT angiography identify coronary lesions that cause ischemia: a direct comparison to fractional flow reserve. *J Am Coll Cardiol Img*. 2015;8:1–10.
  23. Tearney GJ, Regar E, Akasaka T, et al. Consensus standards for acquisition, measurement, and reporting of intravascular optical coherence tomography studies: a report from the International Working Group for Intravascular Optical Coherence Tomography Standardization and Validation. *J Am Coll Cardiol*. 2012;59:1058–1072.
  24. Hoshino M, Yonetsu T, Usui E, et al. Clinical significance of the presence or absence of lipid-rich plaque underneath intact fibrous cap plaque in acute coronary syndrome. *J Am Heart Assoc*. 2019;8:e011820.
  25. Miyamoto Y, Okura H, Kume T, et al. Plaque characteristics of thin-cap fibroatheroma evaluated by OCT and IVUS. *J Am Coll Cardiol Img*. 2011;4:638–646.
  26. Sugiyama T, Yamamoto E, Fracassi F, et al. Calcified plaques in patients with acute coronary syndromes. *J Am Coll Cardiol Interv*. 2019;12:531–540.
  27. Nakajima A, Araki M, Minami Y, et al. Layered plaque characteristics and layer burden in acute coronary syndromes. *Am J Cardiol*. 2022;164:27–33.
  28. Driessen RS, de Waard GA, Stuijzand WJ, et al. Adverse plaque characteristics relate more strongly with hyperemic fractional flow reserve and instantaneous wave-free ratio than with resting instantaneous wave-free ratio. *J Am Coll Cardiol Img*. 2020;13:746–756.
  29. Ando H, Takashima H, Suzuki A, et al. Impact of lesion characteristics on the prediction of optimal poststent fractional flow reserve. *Am Heart J*. 2016;182:119–124.
  30. Sonck J, Collet C, Mizukami T, et al. Motorized fractional flow reserve pullback: accuracy and reproducibility. *Catheter Cardiovasc Interv*. 2020;96:E230–E237.
  31. Li ZY, Taviani V, Tang T, et al. The mechanical triggers of plaque rupture: shear stress vs pressure gradient. *Br J Radiol*. 2009;82(Spec No 1):S39–S45.
  32. Chatzizisis YS, Coskun AU, Jonas M, Edelman ER, Feldman CL, Stone PH. Role of endothelial shear stress in the natural history of coronary atherosclerosis and vascular remodeling: molecular, cellular, and vascular behavior. *J Am Coll Cardiol*. 2007;49:2379–2393.
  33. Genereux P, Madhavan MV, Mintz GS, et al. Ischemic outcomes after coronary intervention of calcified vessels in acute coronary syndromes. Pooled analysis from the HORIZONS-AMI (Harmonizing Outcomes With Revascularization and Stents in Acute Myocardial Infarction) and ACUITY (Acute Catheterization and Urgent Intervention Triage Strategy) trials. *J Am Coll Cardiol*. 2014;63:1845–1854.
  34. Tian J, Dauerman H, Toma C, et al. Prevalence and characteristics of TCFA and degree of coronary artery stenosis: an OCT, IVUS, and angiographic study. *J Am Coll Cardiol*. 2014;64(7):672–680.
  35. Motoyama S, Ito H, Sarai M, et al. Plaque characterization by coronary computed tomography angiography and the likelihood of acute coronary events in mid-term follow-up. *J Am Coll Cardiol*. 2015;66:337–346.
  36. Collet C, Collison D, Mizukami T, et al. Differential improvement in angina and health-related quality of life after PCI in focal and diffuse coronary artery disease. *J Am Coll Cardiol Interv*. 2022;15(24):2506–2518. <https://doi.org/10.1016/j.jcin.2022.09.048>
  37. Chaitman BR, Alexander KP, Cyr DD, et al. Myocardial infarction in the ISCHEMIA trial: impact of different definitions on incidence, prognosis, and treatment comparisons. *Circulation*. 2021;143:790–804.
  38. Yang S, Koo BK, Hwang D, et al. High-risk morphological and physiological coronary disease attributes as outcome markers after medical treatment and revascularization. *J Am Coll Cardiol Img*. 2021;14:1977–1989.
- 
- KEY WORDS** calcification, coronary computed tomography angiography, lipid-rich plaque, optical coherence tomography, pullback pressure gradient, thin-cap fibroatheromas
- 
- APPENDIX** For supplemental tables and a figure, please see the online version of this paper.